



UNSW
A U S T R A L I A

**SCHOOL OF ELECTRICAL ENGINEERING
AND TELECOMMUNICATIONS**

**Achievable Rate Maximization for
IRS-assisted Multiuser Systems**

by

Hongyi Tang

Thesis submitted as a requirement for the degree
Master of Engineering Science (Electrical Engineering)

Submitted: 19th Nov. 2020

Master of Engineering Science (Electrical Engineering)

Abstract

Recently, the commercialization of 5G technology is speeded up in every country. However, each telecom-operator is now definitely managing more than two kinds of telecommunication networks, some might even have three. With the huge overheads of the maintenance, the biggest challenge of the popularization of the 5G is the cost. Besides, owing to the exploration of the extremely high-frequency resources, the coverage capability would be decreased a lot compared to the previous generation network. One possible way is to increase the number of 5G base stations. But a large amount of cost of this solution might slow down the progress of commercialization. Thus, the intelligent reflecting surface was introduced by the researchers to solve this problem. An IRS panel has simple physical structure and low costs, which is able to be easily installed on the walls or the building surfaces. And it can perform as a relay to reflect the signal and improve the quality of the received signal of the users at the edge of the cells and behind the barriers.

Furthermore, comparing to the pure physical reflection, the IRS is working with some beamforming algorithm which can increase the received quality in a certain extend. Thus, this paper investigates a MISO system with IRS and model the system with mathematical equations. Then, introduces some convex optimization methods to solve the beamforming problem of the IRS and discusses the simulation results obtained by solving the non-convex optimization problem.

Acknowledgement

To start with, I would like to show my sincere gratitude to my supervisor, Dr Derrick Kwan Ng. With his large amount of instructive help and guidance, I can eventually understand the complicated principles related to the problems that I met and complete all the mathematical calculations.

And also, many appreciate to my teammates, Chun Bai and Chenyu Gao, who was already completed their project last semester. They also provided me with some help in finding references and learning materials.

Abbreviation

5G	Fifth Generation Communication Network
6G	Sixth Generation Communication Network
MIMO	Multiple Input Multiple Output
SWIPT	Simultaneous Wireless Information and Power Transfer
mmWave	Millimeter Wave
CA	Carrier Aggregation
IRS	Intelligent Reflecting Surface
SINR	Signal to Interference plus Noise Ratio
BS	Base Station
AP	Access Point
SCA	Successive Convex Approximation
AO	Alternative Optimization

Contents

Abstract	I
Acknowledgement	II
Abbreviation	III
Key notation	1
Chapter 1	2
Introduction	2
Chapter 2	4
Background.....	4
The New Generation Communication System.....	4
Intelligent Reflecting Surface	5
Chapter 3	9
System Model	9
Chapter 4	12
Problem formulation.....	12
Solution of the problem	14
Subproblem 1	16
Subproblem 2	19
Alternative optimization	21
Chapter 5	22
Evaluation Results	22
Chapter 6	25
Conclusion	25
Bibliography	Error! Bookmark not defined.
Appendix	36

Key notation

This section is mainly introducing the key mathematical notations appear in this paper. $|\cdot|$ and $\|\cdot\|^2$ denote taking the absolute value of a vector and the l2 Euclidian norm of a vector respectively. $diag(\cdot)$ stands for the diagonal operator. $[\mathbf{X}]_{m,m}$ represents the (m,m) -entry of matrix \mathbf{X} . And \mathbf{x}^T , \mathbf{x}^H denotes the transpose and conjugate transpose of vector \mathbf{x} . Moreover, the $Rank(\cdot)$ and $Tr(\cdot)$ are calculating the rank and the trace of a matrix, respectively. And more commonly, $\mathbb{C}^{M \times N}$ denotes the complex matrix with M rows and N columns. In addition, the set of the N -dimension Hermitian matrices is represented by \mathbb{H}^N . Also, the gradient of the function with respect to the x is represented as $\nabla_x f(x)$. $\mathbf{X} \succcurlyeq \mathbf{0}$ indicates that the matrix \mathbf{X} positive semidefinite. Lastly, for \triangleq and \sim , the meanings should be “defined as” and “distributed as” in this paper.

Chapter 1

Introduction

As the commercialization of the 5G system is currently in full swing, the performance of the system should be strictly guaranteed. The research shows that the number of 5G devices would be increased as 1000 times as before [1]. There are three main cases that should be focused in order to meet the needs of the new generation of the communication system. The mMTC and the eMBB are related to the massive connectivity, large coverage and the high-throughput scenario [2]. Since the 5G system is using the millimeter wave (mmWave) communication, energy consumption and the hardware cost are the main issue for commercial implementation [3]. And according to the theorem mentioned in [2], the ability of a signal to go through the walls is related to the wavelength of the signal. Owing to that the high frequency used for the 5G or B5G, or higher generation communication system, the short wavelength would affect the coverage of the BS significantly [1]. Thus, the IRS was promoted to tackle this issue by providing a cost-efficient and energy-efficient solution. Moreover, uRLLC (ultra-reliable and low-latency communication) is considered to be another typical case of the 5G application scenario. It requires the system to provide reliable performance to support all kinds of real-time services in the future, like the auto-driving and remote surgery applications [4].

Considering the aforementioned 5G's application scenarios, the coverage of the radio signal and the cost efficiency is currently the crucial obstacles to implement the system on a large scale. Hence, the intelligent reflecting surface is now a vital technology that can tackle the issues in a certain extend [5]. With the simple hardware structure, the cost of the IRS panel would be relatively low. In general, the material cost is just around hundred-dollars-level. More importantly, the passive antennas array on the IRS is the key for energy saving. It only needs to be controlled by an IRS controller [6]. On the other hand, the users at the edge of the cells can also receive a high-quality signal with its negative refraction and other properties [6].

In figure (1), a typical IRS system is presented. In general, the system consists of an antenna panel and an IRS controller which is to manipulate the phase shifts of the signal. It can be verified that it is an easily installed system which can be embedded in an indoor wall or any other building's surfaces [5].

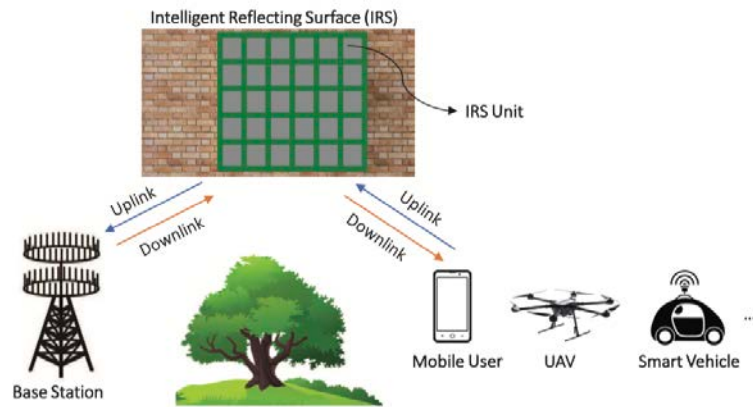


Fig. 1 Communication system with IRS

Cited from J. Zhao's work in 2019 [7]

Furthermore, [8], [9] has also discussed the IRS technology with the high-security requirement. In [8], researchers also take the SWIPT scenario into account to obtain an optimal solution for the secure IRS system. [10], [11] also introduced several methods to optimize the system, such as the channel estimation algorithm and passive beamforming. In this paper, the IRS system with multiple users which also known as MISO system would be discussed. And based on the system model we constructed, the optimal solution would be obtained in ordered to optimize the transmit power and the phase shift matrix and maximize the received signal power at the users.

Chapter 2

Background

The New Generation Communication System

The fifth-generation network (5G) has been deployed worldwide. The high-frequency resources that it uses provides not only the high bit rate but also the massive connectivity and the low latency. However, the wavelength of the radio is related to its frequency. The higher the frequency is, the shorter the wavelength would be [12]. Thus, for the 5G spectrum resources, the wavelength of the radio signal even reaches the millimeter level which means the wall penetration performance would be very poor.

The simple way to fix this problem is to increase the density of base stations and create more and more radio cells. But it would cost much more than the previous communication system because the desiring number of devices that are served by the single base station is way greater than before. In the six-generation (6G), the density of the connected devices is going to reach 10^7 devices per square kilometers [13]. Moreover, the bit rate of the network is required to be in the extremely high level to obtain the low latency, high-reliability features. The public and the organizations are expecting the faster network to be deployed which will be 100 times faster than the previous generation and reaches around 10Gbits/s throughput [2] [14]. Hence, the QoS of the networks should be the principal purpose to be guaranteed. At the meanwhile, the cost of the equipment, as well as the energy efficiency of the system should also be constrained in a reasonable range. MIMO, SWIPT, mmWave, CA and IRS technologies or many other technologies are proposed to meet some technical needs, such as high throughput, better system capacity.

Nevertheless, unlike the previous generation network, owing to the deployment cost of the 5G base station, the application of 5G systems will be business-driven [15]. No operators are affordable to maintain several communication networks at the same time

while the 3G and 4G network is still under maintenance [16]. Some operators in China such as China Union are working on dismantling the GSM base station to support the deployment and development of 5G system [17]. Hence, the current preliminary researches to reduce the cost of the telecommunication system would be vital and they are the keys that pushing the commercialized progress [1] [2] [15].

*Table 1. Capability improvement of 5G over 4G
Cited from Chen's work in 2018*

Key performance index	Value for 5G by ITU	Improvement compared with 4G
Traffic density	10 Tbps/km ²	1000 times
Connection density	1 million/km ²	1000 times
Delay	1 ms (RTT for radio interface)	1/10 times
Peak data rate	10/20 Gbps	100 times
User experience data rate	0.1–1 Gbps or 0.1 Gbps+description	10 times
Mobility	500 km/h	<5 times
Spectrum efficiency	[2/3/5]x	<5 times
Energy efficiency	100x (network)	100 times

Table (1) shows that the expected system loading and the general requirements of the upcoming telecommunication networks.

Intelligent Reflecting Surface

As mentioned in the previous content, in the reality, the 5G signal would be easily blocked by the walls, buildings and the trees or other obstacles. In recent years, more and more researchers start studying the intelligent reflecting surface (IRS) which provides a low-cost method to tackle the issues that the modern telecommunication systems are facing.

The basic concept of the IRS is to reflect the radio signal transmitted from the base station by using some passive antenna array. It can be considered as a MISO system, which receives multiple inputs from the transmitter and then utilizes beamforming to

reflect the desired signal and re-beamforming to the corresponding receiver. A typical IRS system is shown in figure (2), it contains the transmitters, the receivers, the IRS panel and the IRS controller [18].

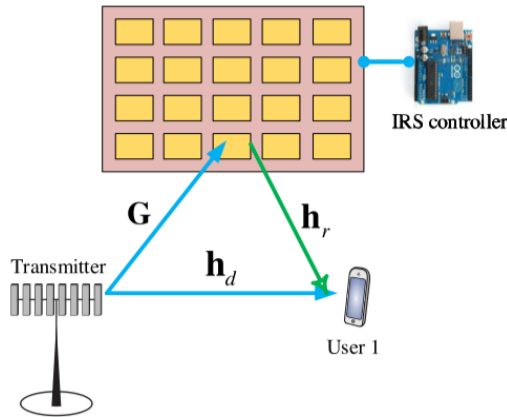


Fig 2. An IRS enhanced multiple antennas system
Cited from J. Zhang's work in 2020 [6]

As presented in figure (3), the IRS panel consists of several meta-atoms which can passively reflect the radio signals to the desired users [6] [18]. Each meta-atom is a low-cost antenna which can perform as the reflector and connected to an IRS controller. In some cases, the meta-atoms would also perform as the energy harvesters in some SWIPT based system.

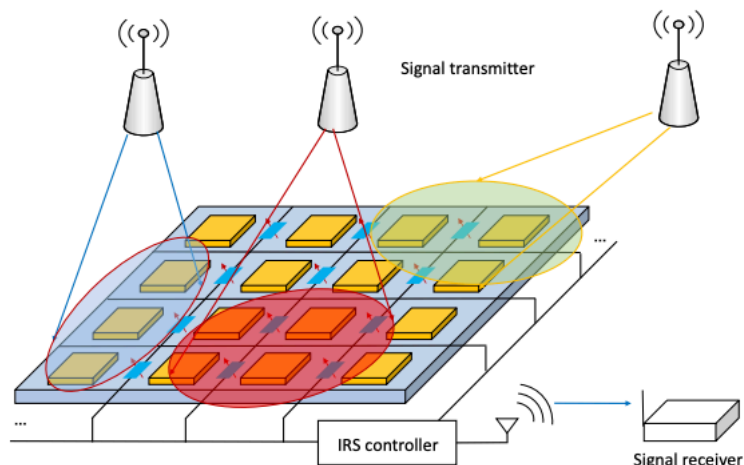


Fig 3. IRS details
Cited from S. Gong's work in 2020 [18]

More importantly, there are many other merits other than the low-cost property of the IRS technology [19] [20]. First of all, the IRS panel is easy installed and energy efficiency, which make it possible to be installed indoors and enhance the signal coverage. Besides, it is able to increase the QoS of the users at the edge of the cells. Since the IRS is reflecting the signal passively, no other noise would be added in the procedure. And it can relatively reduce the interferences from the neighbor cells that affects the users. Thirdly, the system can also be used to increase the physical layer security [20] [21]. By taking the artificial noise and the beam forming algorithm into account, the security is able to get substantial improvement. The simulation results in [9] [20] [22] are presenting the conclusion that with the help of the artificial noise and the appropriate optimization algorithm, the power of the received signals at the eavesdropper's side can dramatically decreased and the overall system performance could be improved in a certain extend.

It can be easily concluded that, the IRS would be an expectable technology that plays a vital role in 5G commercializing progress. As the data shows in table 2, IRS has a lot of potential in the future and more researches should be proposed to improve this technology.

Table 2. Realizing the IRS in the smart radio environment

Cited from S. Gong's work in 2020

Concept/Scheme	Design approach	Application scenario	Validation
Intelligent wall	Switch FSS between ON and OFF to shape the propagation environment	Smart indoor environment for OFDMA system	Extend coverage and improve system performance up to 80% by simulation
ANN-based intelligent wall	Use ANN to explore the optimal setting for controlling the intelligent walls	Smart indoor environment at 2 GHz	Simulations show quick responses to demands and improved performance
Spatial microwave modulator (SMM)	Use a binary-phase state tunable metasurface to manipulate EM waves	SMM fabricated at the 2.47 GHz frequency	Experiments show the capability of improving or cancelling RF signals
Programmable radio environment	Embed low-cost devices in walls to passively reflect active RF signals	Indoor 2.4 GHz Wi-Fi-like communications	Experiments show the efficacy of attenuating or enhancing signal by 26 dB
Programmable wireless environment	Control current distribution over hypersurface tiles to manipulate EM waves	Indoor 60 GHz mmWave communications	Simulations demonstrate significantly improved coverage and received power
Programmable wireless environment	Hypersurface for interference control, security, and distortion mitigation	Indoor 2.4 GHz and 60 GHz communications	Simulations show groundbreaking performance and security potential
Ultra-Massive MIMO	Deploy plasmonic arrays at the transceivers and through the channel	mmWave and THz communications	Significant improvements in communication distance and data rate
Intelligent mirror	Create LOS link by rotating the IRS or electronically changing the wavefront	Free space optical (FSO) communications	Simulations show that building sway for the IRS has either a smaller or larger impact on the channel quality
Physical shaping of propagation medium	Install binary-phase state tunable metasurface inside random environment	2.47 GHz Wi-Fi frequency	Experiments show perfect channel orthogonality, optimal channel diversity, flexible interference suppression

Furthermore, there are many inspired works proposed by previous researchers. Such as [3], the researchers studied the single-user system with IRS and obtained the

optimal solution for the maximum achievable rate. Then a secure system that introduces the artificial noise was discussed in [9]. And the solution to the problem in that paper improves not only the system capacity but also the security compares to other traditional IRS system. In addition, [8] combined the SWIPT system with the IRS and further improve the system performance which enables to extend the battery life of the IoT devices. [18]-[25] are all focused on improving either the security of the IRS system or the energy consumption of the system with various non-convex optimization methods. Hence, based on the previous studies, this paper provides a tight solution for maximizing the channel rate of a multi-user IRS system. And distinct with some of the previous studies, this paper used an optimal method to get a tighter solution of the phase shift matrix rather than directly applied SDR and utilized the Gaussian randomization [3].

Chapter 3

System Model

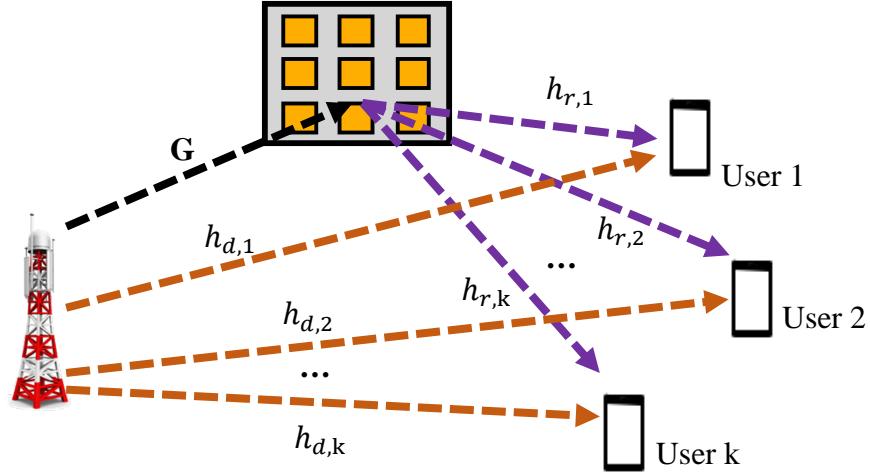


Fig 4. The downlink of the multiuser IRS system

As shown in figure (4), the basic system model is depicted. For each user, the IRS system behaves like a MISO system [23]-[27]. Assuming that there are $N > 1$ antennas used by the transmitter (BS) and M reflectors on the IRS. For user k , $k \in \mathcal{K} \triangleq \{1, \dots, K\}$, where K is the number of users that served by the same base station. $\mathbf{G} \in \mathbb{C}^{M \times N}$ represents the channel matrix between the base station and the IRS. And there are two channels between user k and the base station which are $h_{d,k}$ and the $h_{r,k}$ respectively. And $h_{d,k} \in \mathbb{C}^{N \times 1}$ denotes the channel vector between the direct path between the BS and the user while $h_{r,k} \in \mathbb{C}^{M \times 1}$ stands for the channel vector between the IRS and the user. Then the received power at the user k could be presented as y_k ,

$$y_k = (h_{r,k}^H \Phi \mathbf{G} + h_{d,k}^H) \left(\sum_{k=0}^K w_k s_k \right) + n_k \quad (1)$$

Simplify the formula (1) by using the x which is on behalf of the mixed signal that received by the user k . And $s_k \in \mathbb{C}$ is the transmitted symbols from the BS to the user. In this paper, the physical layer security would not be discussed and the AN

should not be added at the transmitter [8] [9] [28] and we assume that the modulation noise or other noises introduce at the transmitter and the receiver are zero.

And (1) could be rewritten in a form with x :

$$y_k = h_k^H x + n_k \quad (2)$$

where, $x = \sum_{k=0}^K w_k s_k$, $h_k^H = h_{rk}^H \Phi \mathbf{G} + h_{dk}^H$.

Furthermore, $\Phi = \text{diag}\{\beta_1 e^{j\theta_1}, \beta_2 e^{j\theta_2}, \dots, \beta_M e^{j\theta_M}\}$ and $\theta_m \in [0, 2\pi]$ for $m \in (1, \dots, M)$ represent the phase shift matrix and the phase shift value respectively. In general, β_m should be equal to 1 which can make sure that the beam forming of the IRS would only adjust the phase of the desired signal and not changing the amplitude of the original signal [3]. Inspired by the assumption in [3], we assuming that the linear beamforming is used by the BS and $w_k \in \mathbb{C}^{N \times 1}$ denotes the beamforming vector at the base station side. Besides, $n_k \sim \mathcal{CN}(0, \sigma_{n_k}^2)$ is considered as the additive Gaussian white noise which might be introduced by the wireless circumstance received by user k [9]. And $\sigma_{n_k}^2$ represents the energy of the noise in general [29] [30].

Then the SINR measured at the receiver k can be expressed as (3) [31] [32]. The irrelevant signals that received by user k are considered as the interference:

$$SINR_k = \frac{|h_k^H w_k|^2}{\sum_{i \neq k}^N |h_k^H w_i|^2 + \sigma_{n_k}^2} \quad (3)$$

Based on the Shannon formula [33], the channel capacity between base station and user k could be obtained:

$$C_k = \log(1 + SINR_k) = \log\left(1 + \frac{|h_k^H w_k|^2}{\sum_{i \neq k}^N |h_k^H w_i|^2 + \sigma_{n_k}^2}\right) \quad (4)$$

C_k stands for the achievable rate (bit/s/Hz) measured at the user k [9]. In order to study the multiuser system and prevent the network eventually just serving one user [34]-[36], the sum of the C_k for $\forall k$ should be discussed at the following chapters.

Chapter 4

Problem formulation

According to the previous chapter, the optimization problem of this paper could be summarized as finding the maximum sum of the achievable information rate of all k users. And as shown in table 3, (6) illustrates the objective of the problem of this paper, and it can obtain the optimal capability of the system by using proper beamforming vector w_k and the phase shift matrix Φ .

Table 3. Problem formulation

$\underset{\Phi, w_k}{\text{maximize}} \sum_{k \in \mathcal{K}} \log \left(1 + \frac{ h_k^H w_k ^2}{\sum_{i \neq k}^N h_k^H w_i ^2 + n_k^2} \right) \quad (P1)$
<p>s.t.:</p> $C1: \sum_k \ w_k\ ^2 \leq P_{max},$ $C2: SINR_k \geq \gamma_k, \forall k \in \mathcal{K}$ $C3: [\Phi]_{m,m} = 1, \forall m,$ $C4: 0 \leq \theta_m \leq 2\pi, \forall m,$

where P_{max} represents for the max transmit power of the BS/AP and the γ_k is considered as the minimum received signal quality for each use.

There are three constrains in table 3 in total. $C1$ indicates that the total beamforming power should be constrained in the range of the transmitter's energy capability. Then $C2$ is to guarantee the user experience and define a minimum SINR value that expected to be obtained by each receiver. Moreover, $C3$ illustrates that the phase shift element should only change the phase of the signal but not taking any changes on the amplitude or the frequency [37]-[41]. And last but not least, $C4$ constrains the

phase shift value in the range of 2π . And it can be easily concluded that, owing to the denominator of the SINR, (P1) and C2 are not convex. Hence, the alternating optimization algorithm and SCA and other convex optimization methods would be introduced in the next section to solve the problem.

Solution of the problem

The purpose of this paper is to maximize the system capacity by jointly adjusting and optimizing the Φ , w_k which denotes the transmit beamforming at the BS side and the reflect beamforming at the IRS side respectively. However, in the formulas of (P1), the Φ , w_k are coupled and the nonconcave constraint C2. Even though C1, C3, C4 are all convex, the objective function is a non-concave problem.

Before we start tackling the optimization problem (P1), the formulas should be firstly simplified. We firstly define $\mathbf{W}_k = w_k \mathbf{w}_k^H$, $\mathbf{H}_{r,k} = \text{diag}(h_{r,k}^H) \mathbf{G}$, $\mathbf{H}_{d,k} = \text{diag}(h_{d,k}^H)$ and $\mathbf{u} = [e^{j\theta_1}, e^{j\theta_2}, \dots, e^{j\theta_m}]^H$. Hence, the $SINR_k$ could be rewritten as:

$$SINR_k = \frac{\text{Tr}[\mathbf{W}_k(\mathbf{H}_{r,k}^H \mathbf{u} \mathbf{u}^H \mathbf{H}_{r,k} + \mathbf{H}_{d,k}^H \mathbf{H}_{d,k})]}{\sum_{i \neq k}^N \text{Tr}[\mathbf{W}_i(\mathbf{H}_{r,k}^H \mathbf{u} \mathbf{u}^H \mathbf{H}_{r,k} + \mathbf{H}_{d,k}^H \mathbf{H}_{d,k})] + n_k^2} \quad (5)$$

Define F_1, F_2 as the following formulas:

$$F_1(\mathbf{u}, \mathbf{W}_k) = \sum_{k \in \mathcal{K}} \log \left(\sum_{i \neq k}^N \text{Tr}[\mathbf{W}_i(\mathbf{H}_{r,k}^H \mathbf{u} \mathbf{u}^H \mathbf{H}_{r,k} + \mathbf{H}_{d,k}^H \mathbf{H}_{d,k})] + \text{Tr}[\mathbf{W}_k(\mathbf{H}_{r,k}^H \mathbf{u} \mathbf{u}^H \mathbf{H}_{r,k} + \mathbf{H}_{d,k}^H \mathbf{H}_{d,k})] + n_k^2 \right) \quad (6)$$

$$F_2(\mathbf{u}, \mathbf{W}_k) = \sum_{k \in \mathcal{K}} \log \left(\sum_{i \neq k}^N \text{Tr}[\mathbf{W}_i(\mathbf{H}_{r,k}^H \mathbf{u} \mathbf{u}^H \mathbf{H}_{r,k} + \mathbf{H}_{d,k}^H \mathbf{H}_{d,k})] + n_k^2 \right) \quad (7)$$

Hence, the channel capacity could be reformulated and (P1) is transformed into (P2) by applying F_1 and F_2 . According to the definition of \mathbf{u} and \mathbf{W}_k , they represent the new optimization parameters instead of Φ and w_k .

And now, \mathcal{C}_k can be reformulated as $\mathcal{C}_k = F_1 - F_2$. The simplified problem with F_1 and F_2 in terms of \mathbf{u} and \mathbf{W}_k shows in table 4.

Table 4. The Problem formulation in terms of \mathbf{u} and \mathbf{W}_k

	$\text{maximize}_{\mathbf{u}, \mathbf{W}_k \in \mathbb{H}^N} F_1(\mathbf{u}, \mathbf{W}_k) - F_2(\mathbf{u}, \mathbf{W}_k) \quad (P2)$
s.t.:	$C1: \sum_k \text{Tr}(\mathbf{W}_k) \leq P_{max},$ $C2: \text{SINR}_k \geq \gamma_k, \forall k \in \mathcal{K},$ $C3: u_m = 1, \forall m,$ $C4: 0 \leq \theta_m \leq 2\pi, \forall m,$ $C5: \text{Rank}(\mathbf{W}_k) = 1, \forall k$ $C7: \mathbf{W}_k \succeq 0$

$C5$ and $C7$ are proposed to make sure that $\mathbf{W}_k = w_k w_k^H$ can still get the correct results after optimization [9] [42]-[45]. u_m denotes the m th element of the updated beamforming vector \mathbf{u} . However, owing to the coupling of the \mathbf{u} and \mathbf{W}_k , the non-convex constraints $C2$, $C3$, and $C5$, make (P2) still be non-concave. Then in the following sections, the alternative optimization (AO) and successive convex approximation (SCA) would be implemented for computational feasibility and decoupling. The optimal \mathbf{u} and \mathbf{W}_k are going to be solved iteratively with other one fixed [46]-[50]. Thus, the problem now could be separated into two subproblems with alternative optimization.

Subproblem 1

First and foremost, for a fixed value of \mathbf{W}_k , the problem (P2) can be reduced to the problem presented in table 5.

Table 5. The Problem formulation with fixed \mathbf{W}_k

	$\underset{\mathbf{u}}{\text{maximize}} F_1(\mathbf{u}) - F_2(\mathbf{u})$	(P3)
s.t.:	$C1: SINR_k \geq \gamma_k, \forall k \in \mathcal{K}$	
	$C2: u_m = 1, \forall m,$	
	$C3: 0 \leq \theta_m \leq 2\pi, \forall m,$	

Now the constraints C1, C3 are all convex functions. Even though the F_1 and F_2 are now concave, because of the subtraction operator between them and the constraint C2, (P3) is still not concave. And SDR is not able to make the solution tight. Thus, SDP is also needed for solving the optimization problem.

Then define $\Psi = \mathbf{u}\mathbf{u}^H$. In order to make this formula holds after the optimization. According to the matrix property $\Psi = \sum_{i=1}^r \alpha_i \phi_i \phi_i^H$, where $r = Rank(\Psi)$, then we should introduce two new constraints to the problem which are $\Psi \succeq 0$ and $Rank(\Psi) = 1$ to satisfy the requirement. However, it is obvious that the rank-one constraint is not convex and there is no way to proof it holds under any circumstance. In general, SDR and Gaussian randomization would be used to obtain the solution [3]. But this cannot be guaranteed that the solution we got is tight. Thus, we can rewrite the rank-one constrain in another form:

$$Tr(\Psi) - \lambda_{max}(\Psi) \leq 0 \quad (8)$$

Nonetheless, the (8) is still not convex since $\lambda_{max}(\Psi)$ is a non-linear convex function. Thus, to make this constrain convex, SCA should be used. The principle is

that although the result of the subtraction between two concave functions might not lead to a concave problem, if we can translate $\lambda_{max}(\Psi)$ to a linear function, the problem would be convex eventually [56]-[60]. We define $\tilde{\lambda} = \lambda_{max}(\Psi) + Tr[\nabla_{\lambda}\lambda_{max}(\Psi)(\lambda - \lambda^i)]$, where $\tilde{\lambda}$ denotes for the first order Taylor expansion of $\lambda_{max}(\Psi)$ at any feasible point λ^i . Then (8) is able to be rewritten as:

$$Tr(\Psi) - \tilde{\lambda} \leq 0 \quad (9)$$

And (9) can be used as the convex constraint. Hence, (P3) can be transformed into (P4):

Table 6. The Problem formulation in terms of Ψ

	$\underset{\Psi}{\text{maximize}} F_1(\Psi) - F_2(\Psi) \quad (P4)$
s.t.:	$C1: SINR_k \geq \gamma_k, \forall k \in \mathcal{K}$
	$C2: \Psi_{n,n} = 1, n = 1, 2, \dots, N + 1$
	$C3: \Psi \succeq 0$
	$C4: Tr(\Psi) - \tilde{\lambda} \leq 0$

For (P4), the only remaining non-convex function is the problem formula. In order to make the (P4) concave, we need to use SCA, i.e., using Taylor expansion for $F_2(\Psi)$ to approximate it as a linear function [61]-[65]. Similar to the aforementioned steps, we firstly define $\widetilde{F}_2(\Psi, \Psi^i)$ which is the approximation function at the feasible point Ψ^i .

And $F_2(\Psi) \leq \widetilde{F}_2(\Psi, \Psi^i) = F_2(\Psi^i) + Tr[(\nabla_{\Psi} F_2(\Psi^i))^H(\Psi - \Psi^i)]$.

Table 7. The Problem formulation after applying the SCA on (P4)

$$\underset{\Psi}{\text{maximize}} F_1(\Psi) - \widetilde{F}_2(\Psi, \Psi^i) \quad (P5)$$

s. t.:

$$C1: SINR_k \geq \gamma_k, \forall k \in \mathcal{K}$$

$$C2: \Psi_{n,n} = 1, n = 1, 2, \dots, N + 1$$

$$C3: \Psi \succeq 0$$

$$C4: Tr(\Psi) - \tilde{\lambda} \leq 0$$

Eventually, for the above convex optimization problem (P5), the optimal solution is able to be obtained by applying algorithm 1.

Algorithm 1: Successive Convex Approximation Algorithm For obtaining Ψ^*

- 1: Initialize the iteration index, $i = 1$, and the maximum iteration time i_{max} .
- 2: Give the corresponding W_k .
- 3: **repeat**
- 4: Solve (P5) with given feasible point Ψ^i and store the temporary solution of Ψ .
- 5: Set $i = i + 1$ and $\Psi^i = \Psi$
- 6: **until** convergence **or** i equals to i_{max}

$$\Psi^* = \Psi^i$$

Subproblem 2

For a given \mathbf{u} , the problem (P2) can be reformulated as following:

Table 7. The Problem formulation with fixed \mathbf{u}

	$\underset{\mathbf{W}_k}{\text{maximize}} F_1(\mathbf{W}_k) - F_2(\mathbf{W}_k) \tag{P6}$	
s.t.:	$C1: \sum_k Tr(\mathbf{W}_k) \leq P_{max}$	
	$C2: SINR_k \geq \gamma_k, \forall k \in \mathcal{K}$	
	$C3: Rank(\mathbf{W}_k) = 1, \forall k$	
	$C4: \mathbf{W}_k \succeq 0$	

Since it can be easily proofed that (P6) is still not concave. Hence, SCA method should be used to make (P6) a concave function. In order to implement the SCA, we first define approximation function of F_2 similar to subproblem 1 and represents it as \widetilde{F}_2 . We translate the F_2 to a linear function and for any feasible point \mathbf{W}_k^i and the differentiable concave function $F_2(\mathbf{W}_k)$, we can obtain the following formula by using the first order Taylor expansion [66]-[68]:

$$\begin{aligned}
 F_2(\mathbf{W}_k) &\leq F_2(\mathbf{W}_k^i) + Tr \left[(\nabla_{\mathbf{W}_k} F_2(\mathbf{W}_k^i))^H (\mathbf{W}_k - \mathbf{W}_k^i) \right] \\
 &\triangleq \widetilde{F}_2(\mathbf{W}_k, \mathbf{W}_k^i)
 \end{aligned} \tag{10}$$

However, the existence of rank-one constraint C3 makes the problem hard to be tackled even after applying the SCA. We can further drop the rank-one constraint by applying SDR to get the tight solution of (P6) [9][66]. The rank-one property of the beamforming matrix \mathbf{W}_k is proofed by using KKT conditions [69] which is presented in the appendix.

Then (P6) could be formulated as below:

Table 8. The Problem formulation after applying the SCA on (P6)

	$\underset{\mathbf{u}}{\text{maximize}} F_1(\mathbf{W}_k) - \widetilde{F}_2(\mathbf{W}_k, \mathbf{W}_k^i) \quad (P7)$
s.t.:	$C1: \sum_k Tr(\mathbf{W}_k) \leq P_{max}$
	$C2: SINR_k \geq \gamma_k, \forall k \in \mathcal{K}$
	$C3: \mathbf{W}_k \succeq 0$

Hence, (P7) is able to be summarized as algorithm 2 which leads to a tight optimal solution for \mathbf{W}_k^* .

Algorithm 2: Successive Convex Approximation Algorithm For obtaining \mathbf{W}_k^*

- 1: Initialize the iteration index, $j = 1$, and the maximum iteration time j_{max} .
- 2: Give the corresponding \mathbf{u} .
- 3: **repeat**
- 4: Solve (P7) with given feasible point \mathbf{W}_k^j and store the temporary solution of \mathbf{W}_k .
- 5: Set $j = j + 1$ and $\mathbf{W}_k^j = \mathbf{W}_k$
- 6: **until** convergence **or** j equals to j_{max}

$$\mathbf{W}_k^* = \mathbf{W}_k^j$$

Alternative optimization

Last but not least, combining algorithm 1 and algorithm 2 to tackle (P2) iteratively. The optimal solution of parameters W_k^* and Ψ^* can be obtained by the algorithm 3 which is shown below.

Algorithm 3: Alternative optimization for obtaining W_k^* and Ψ^*

- 1: Initialize the iteration index, $t = 1$, and the maximum iteration time t_{max} .
 - 2: Give the initial point $W_k^{(t)}$.
 - 3: **repeat**
 - 4: Solve (P3) by applying **Algorithm 1** with given $W_k^{(t)}$ and store the current solution as $\Psi^{(t)}$.
 - 5: Solve (P7) by applying **Algorithm 2** with the previously obtained $\Psi^{(t)}$ and store the current solution as $W_k^{(t+1)}$
 - 5: Set $t = t + 1$
 - 6: **until** convergence **or** t equals to t_{max}
- Output the optimal solution with $W_k^* = W_k^{(t)}$ and $\Psi^* = \Psi^{(t)}$
-

Chapter 5

Evaluation Results

In this section, the simulation results are going to be proposed with different system configurations and operating circumstance. The overall system configuration is presented in table (9). And we take some of the values used in [74] for our simulation. In addition, the users are located in a circle with a radius of one meter. And the distances of the BS-user link, BS-IRS link and IRS-user link are all defined as variables.

Table 9. System parameters

System bandwidth	200kHz
Noise power, $\sigma_{n_k}^2$	-110dBm
Antenna gains at receiving side	0 dBi
Antenna gains at transmitting side	10dBi
Phase shifter bit resolution	3 bits
Path loss exponent of BS-IRS link	2.2
Path loss exponent of IRS-user link	2.2
Fading coefficients	BS-user link=0, BS-IRS link=2, IRS-user link=2

The simulation was separated into two main subsections. The first part is in order to study the system performance with various IRS configuration and different maximum transmit power values. On the other hand, the second section is mainly to discover the influence of the distance and the number of IRS elements.

First and foremost, in the first simulation, we applied four antenna configurations which is presented in the legend of the diagram. And the results show the performance improvement of the IRS system comparing to the normal system with four users. Moreover, it also points out that the numbers of antennas would bring positive impact to the system.

It is noteworthy that in the illustration of figure (5), N_T represents the antenna number of the transmitter and the M denotes the number of IRS elements. In figure (5), with the same number of antennas at the transmitter side, it is obvious that the system with IRS can provide a relatively high performance-gain comparing to the normal system with no IRS. Nearly provides 4dBm improvement in average. And with more antennas equipped at the transmitter, the higher system throughput would be reached although more power would be consumed. And in general, the system performance gain would not increase dramatically while the number of antennas keeps adding up. Furthermore, as shown in figure 5, the improvement between the blue line and the red line is much smaller than the improvement between the red line and the yellow line. Thus, it can be concluded that, with the IRS, the users in the distance are able to obtain the higher-level service quality. Or, remaining the same received signal quality with less transmit power.

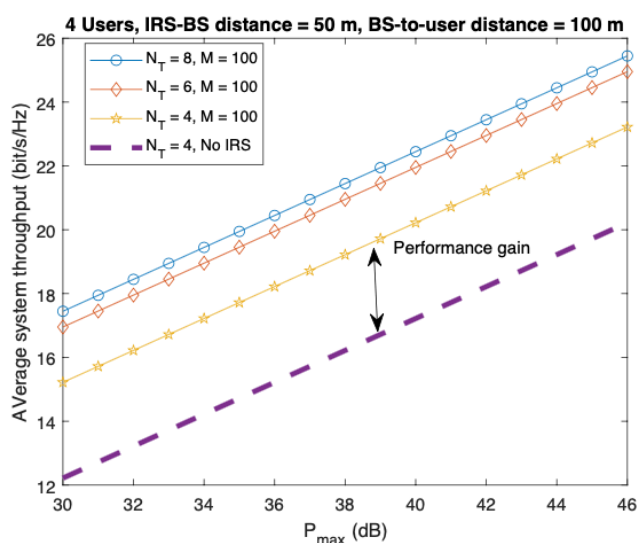


Fig.5 average system throughput versus maximum transmit power (dB) with different sets of N_T and M

For the second simulation, we still used four users in the system and constrained the maximum transmitted power to 30dBm. The system performance can be concluded by analyzing the average throughput rate of the network.

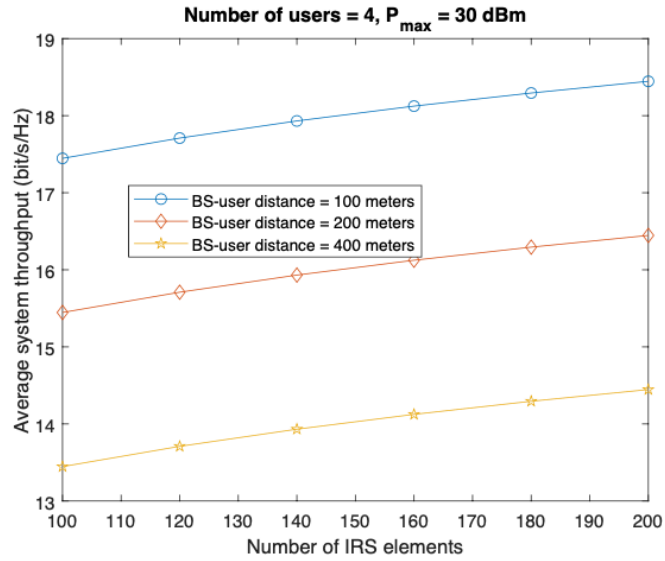


Fig.6 Average system throughput versus number of IRS elements with different distance

In figure (6), the average throughput of the system keeps increasing along with the increment of the number of IRS elements. However, as the number of IRS element grows, the system rate is increasing logarithmic instead of linearly. In the meanwhile, the distance would affect the user experience. As we can see in the diagram, the average throughputs of the users at different distances are various. The users within 100 meters coverage can achieve the highest transmission rate. And the achievable rate is going to be decreased 2 bit/s/Hz for every 100 meters further. Besides, it also shows that with more IRS elements, this issue can be relieved in a certain extend.

Chapter 6

Conclusion

This paper studied a basic method to optimize the system performance of a typical IRS based MISO system. And it mainly focuses on downlink improvement. In the aforementioned solution section, various typical non-convex optimization methods were used. The SCA, AO and SDR were all used to tackle the non-convex optimal problem. And the simulation outcomes present that the method we proposed is feasible and effective for the IRS system. It reveals that in the 5G application, for the developers who want to improve the experience of the users at the edge of the cells, they can consider the IRS as a lower cost and effective way to achieve their objectives.

Besides, for the commercialized implementation in the future, many other advanced non-convex optimization techniques such as oblique manifold optimization and Dinkelbach's method could also be applied for obtaining the more accurate solution of the phase shift matrix and the beamforming vectors of the system. And the techniques that mentioned in this paper operates with some assistant techniques, such as the transmitted power minimization and the energy harvesting techniques [22] [72], a much more robust and reliable system is going to be achieved. Furthermore, artificial noise can be widely used for maintaining the security of the communication system [28].

All in all, the proposition of the IRS system brings a more feasible solution to the telecommunication system for tackling the current issues. And hopefully that the overall system setup procedures mentioned in this paper could inspire other researchers to get involved.

References

- [1] X. Chen, D. W. K. Ng, W. Yu, E. G. Larsson, N. Al-Dhahir and R. Schober, "Massive Access for 5G and Beyond," in *IEEE Journal on Selected Areas in Communications*, doi: 10.1109/JSAC.2020.3019724.
- [2] Q. Wu, G. Y. Li, W. Chen, D. W. K. Ng and R. Schober, "An Overview of Sustainable Green 5G Networks," in *IEEE Wireless Communications*, vol. 24, no. 4, pp. 72-80, Aug. 2017, doi: 10.1109/MWC.2017.1600343.
- [3] Wu, Q. and Zhang, R, "Intelligent Reflecting Surface Enhanced Wireless Network via Joint Active and Passive Beamforming". *IEEE Transactions on Wireless Communications*, 2019, 18(11), pp.5394-5409.
- [4] Z. Li, M. A. Uusitalo, H. Shariatmadari and B. Singh, "5G URLLC: Design Challenges and System Concepts," 2018 15th International Symposium on Wireless Communication Systems (ISWCS), Lisbon, 2018, pp. 1-6, doi: 10.1109/ISWCS.2018.8491078.
- [5] G. Yu, X. Chen, C. Zhong, D. W. K. Ng and Z. Zhang, "Design, Analysis, and Optimization of a Large Intelligent Reflecting Surface-Aided B5G Cellular Internet of Things," in *IEEE Internet of Things Journal*, vol. 7, no. 9, pp. 8902-8916, Sept. 2020, doi: 10.1109/JIOT.2020.2996984.
- [6] J. Zhang, E. Björnson, M. Matthaiou, D. W. K. Ng, H. Yang and D. J. Love, "Prospective Multiple Antenna Technologies for Beyond 5G," in *IEEE Journal on Selected Areas in Communications*, vol. 38, no. 8, pp. 1637-1660, Aug. 2020, doi: 10.1109/JSAC.2020.3000826.
- [7] J. Zhao and Y. Liu, "A Survey of Intelligent Reflecting Surfaces (IRSs): Towards 6G Wireless Communication Networks", 2019. Available: <https://www.researchgate.net/publication/334207323>.

- [8] J. Liu, K. Xiong, Y. Lu, D. W. K. Ng, Z. Zhong and Z. Han, "Energy Efficiency in Secure IRS-Aided SWIPT," in *IEEE Wireless Communications Letters*, doi: 10.1109/LWC.2020.3006837.
- [9] D. Xu, X. Yu, Y. Sun, D. W. K. Ng and R. Schober, "Resource Allocation for Secure IRS-Assisted Multiuser MISO Systems," 2019 IEEE Globecom Workshops (GC Wkshps), Waikoloa, HI, USA, 2019, pp. 1-6, doi: 10.1109/GCWkshps45667.2019.9024490.
- [10] Y. Gao, J. Xu, W. Xu, D. W. K. Ng and M. -S. Alouini, "Distributed IRS with Statistical Passive Beamforming for MISO Communications," in *IEEE Wireless Communications Letters*, doi: 10.1109/LWC.2020.3024952.
- [11] Z. Wang, L. Liu and S. Cui, "Channel Estimation for Intelligent Reflecting Surface Assisted Multiuser Communications: Framework, Algorithms, and Analysis", *IEEE Transactions on Wireless Communications*, pp. 1-1, 2020. Available: 10.1109/twc.2020.3004330.
- [12] W. Zhang, J. Xu, W. Xu, D. W. K. Ng and H. Sun, "Cascaded Channel Estimation for IRS-assisted Mmwave Multi-antenna with Quantized Beamforming," in *IEEE Communications Letters*, doi: 10.1109/LCOMM.2020.3028878.
- [13] J. G. Andrews, S. Buzzi, W. Choi, S. V. Hanly, A. Lozano, A. C. Soong, and J. C. Zhang, "What will 5G be?" *IEEE J. Sel. Areas Commun.*, vol. 32, no. 6, pp. 1065-1082, Jun. 2014.
- [14] Q. Wu, G. Y. Li, W. Chen, and D. W. K. Ng, "Energy-efficient small cell with spectrum-power trading," *arXiv preprint arXiv:1608.03178*, 2016.
- [15] Anwer Al-Dulaimi; Xianbin Wang; Chih-Lin I, "Introduction," in *5G Networks: Fundamental Requirements, Enabling Technologies, and Operations Management*, IEEE, 2018, pp.1-12, doi: 10.1002/9781119333142.ch0.

- [16] M. Shafi et al., "5G: A Tutorial Overview of Standards, Trials, Challenges, Deployment, and Practice," in *IEEE Journal on Selected Areas in Communications*, vol. 35, no. 6, pp. 1201-1221, June 2017, doi: 10.1109/JSAC.2017.2692307.
- [17] Chen, S., Kang, S. "A tutorial on 5G and the progress in China," in *Frontiers Inf Technol Electronic Eng* 19, 309–321 (2018). <https://doi.org/10.1631/FITEE.1800070>
- [18] S. Gong et al., "Towards Smart Wireless Communications via Intelligent Reflecting Surfaces: A Contemporary Survey," in *IEEE Communications Surveys & Tutorials*, doi: 10.1109/COMST.2020.3004197.
- [19] G. Zhou, C. Pan, H. Ren, K. Wang and A. Nallanathan, "Intelligent Reflecting Surface Aided Multigroup Multicast MISO Communication Systems," in *IEEE Transactions on Signal Processing*, vol. 68, pp. 3236-3251, 2020, doi: 10.1109/TSP.2020.2990098.
- [20] Q. Wu and R. Zhang, "Towards Smart and Reconfigurable Environment: Intelligent Reflecting Surface Aided Wireless Network," in *IEEE Communications Magazine*, vol. 58, no. 1, pp. 106-112, January 2020, doi: 10.1109/MCOM.001.1900107.
- [21] X. Yu, D. Xu, Y. Sun, D. W. K. Ng and R. Schober, "Robust and Secure Wireless Communications via Intelligent Reflecting Surfaces," in *IEEE Journal on Selected Areas in Communications*, doi: 10.1109/JSAC.2020.3007043.
- [22] J. Liu, K. Xiong, Y. Lu, D. W. K. Ng, Z. Zhong and Z. Han, "Energy Efficiency in Secure IRS-Aided SWIPT," in *IEEE Wireless Communications Letters*, doi: 10.1109/LWC.2020.3006837.
- [23] D. W. K. Ng, R. Schober and H. Alnuweiri, "Power efficient MISO beamforming for secure layered transmission," 2014 *IEEE Wireless Communications and Networking Conference (WCNC)*, Istanbul, 2014, pp. 422-427, doi: 10.1109/WCNC.2014.6952045.

- [24] J. Dang, Z. Zhang and L. Wu, "Joint beamforming for intelligent reflecting surface aided wireless communication using statistical CSI," in *China Communications*, vol. 17, no. 8, pp. 147-157, Aug. 2020, doi: 10.23919/JCC.2020.08.012.
- [25] S. Hong, C. Pan, H. Ren, K. Wang and A. Nallanathan, "Artificial-Noise-Aided Secure MIMO Wireless Communications via Intelligent Reflecting Surface," in *IEEE Transactions on Communications*, doi: 10.1109/TCOMM.2020.3024621.
- [26] L. Zhang, Y. Wang, W. Tao, Z. Jia, T. Song and C. Pan, "Intelligent Reflecting Surface Aided MIMO Cognitive Radio Systems," in *IEEE Transactions on Vehicular Technology*, doi: 10.1109/TVT.2020.3011308.
- [27] I. Chatzigeorgiou, "The Impact of 5G Channel Models on the Performance of Intelligent Reflecting Surfaces and Decode-and-Forward Relaying," 2020 IEEE 31st Annual International Symposium on Personal, Indoor and Mobile Radio Communications, London, United Kingdom, 2020, pp. 1-4, doi: 10.1109/PIMRC48278.2020.9217321.
- [28] M. A. Saeidi and M. J. Emadi, "IRS-based Secrecy Rate Analysis in Presence of an Energy Harvesting Eavesdropper," 2020 Iran Workshop on Communication and Information Theory (IWCIT), Tehran, Iran, 2020, pp. 1-5, doi: 10.1109/IWCIT50667.2020.9163399.
- [29] A. Khalili and D. W. K. Ng, "Energy and Spectral Efficiency Tradeoff in OFDMA Networks via Antenna Selection Strategy," 2020 IEEE Wireless Communications and Networking Conference (WCNC), Seoul, Korea (South), 2020, pp. 1-6.
- [30] M. Robot Mili, A. Khalili, n. mokari, S. Wittevrongel, D. W. K. Ng and H. Steendam, "Tradeoff Between Ergodic Energy Efficiency and Spectral Efficiency in D2D Communications Under Rician Fading Channel," in *IEEE Transactions on Vehicular Technology*.

- [31] W. Yan, X. Yuan, Z. -Q. He and X. Kuai, "Passive Beamforming and Information Transfer Design for Reconfigurable Intelligent Surfaces Aided Multiuser MIMO Systems," in *IEEE Journal on Selected Areas in Communications*, vol. 38, no. 8, pp. 1793-1808, Aug. 2020, doi: 10.1109/JSAC.2020.3000811.
- [32] L. Zhang, Y. Wang, W. Tao, Z. Jia, T. Song and C. Pan, "Intelligent Reflecting Surface Aided MIMO Cognitive Radio Systems," in *IEEE Transactions on Vehicular Technology*, doi: 10.1109/TVT.2020.3011308.
- [33] Yan-liang Jin, Hao-jie Lin, Huimin-Chen and Zhu-ming Zhang, "Explanation of Shannon formula for the UNB communication," *IET 2nd International Conference on Wireless, Mobile and Multimedia Networks (ICWMMN 2008)*, Beijing, CHina, 2008, pp. 33-36, doi: 10.1049/cp:20080930.
- [34] B. Zheng, Q. Wu and R. Zhang, "Intelligent Reflecting Surface-Assisted Multiple Access With User Pairing: NOMA or OMA?," in *IEEE Communications Letters*, vol. 24, no. 4, pp. 753-757, April 2020, doi: 10.1109/LCOMM.2020.2969870.
- [35] C. You, B. Zheng and R. Zhang, "Fast Beam Training for IRS-Assisted Multiuser Communications," in *IEEE Wireless Communications Letters*, doi: 10.1109/LWC.2020.3005980.
- [36] D. Xu, X. Yu, Y. Sun, D. W. K. Ng and R. Schober, "Resource Allocation for IRS-assisted Full-Duplex Cognitive Radio Systems," in *IEEE Transactions on Communications*, doi: 10.1109/TCOMM.2020.3020838.
- [37] Z. Yan, M. Kang, C. Li, B. Wei and X. Song, "De-re-coupling Modulation Method of Double-rising-edge Phase-shifted SPWM for Current-Source Matrix Rectifier," *2018 IEEE International Power Electronics and Application Conference and Exposition (PEAC)*, Shenzhen, 2018, pp. 1-6, doi: 10.1109/PEAC.2018.8590272.
- [38] U. Vargas, A. Ramirez and E. Karami, "Reformulating Phase-Shifting Property in Dynamic Harmonic Domain: Time-Periodic Case," in *IEEE Transactions on Smart Grid*, vol. 10, no. 3, pp. 3498-3500, May 2019, doi: 10.1109/TSG.2019.2899759.

- [39] V. Ranjan, N. Singh, V. P. Singh and S. B. Singh, "Commutation Problem of Single Phase Matrix Converter with PWM Phase Shift Dead Time Technique," 2018 International Conference on Power Energy, Environment and Intelligent Control (PEEIC), Greater Noida, India, 2018, pp. 44-49, doi: 10.1109/PEEIC.2018.8665420.
- [40] H. Fu, S. Feng, W. Tang and D. W. K. Ng, "Robust Secure Beamforming Design for Two-user Downlink MISO Rate-Splitting Systems," in *IEEE Transactions on Wireless Communications*, doi: 10.1109/TWC.2020.3021725.
- [41] Z. Chen, Z. Ding, P. Xu, X. Dai, J. Xu and D. W. K. Ng, "Comment on "Optimal Precoding for a QoS Optimization Problem in Two-User MISO-NOMA Downlink"," in *IEEE Communications Letters*, vol. 21, no. 9, pp. 2109-2111, Sept. 2017, doi: 10.1109/LCOMM.2017.2707491.
- [42] B. Matthiesen, E. Björnson, E. De Carvalho and P. Popovski, "Intelligent Reflecting Surface Operation under Predictable Receiver Mobility: A Continuous Time Propagation Model," in *IEEE Wireless Communications Letters*, doi: 10.1109/LWC.2020.3024781.
- [43] L. Dong and H. Wang, "Enhancing Secure MIMO Transmission via Intelligent Reflecting Surface," in *IEEE Transactions on Wireless Communications*, doi: 10.1109/TWC.2020.3012721.
- [44] H. Niu and L. Ni, "Intelligent Reflect Surface aided Secure Transmission in MIMO Channel with SWIPT," in *IEEE Access*, doi: 10.1109/ACCESS.2020.3032759.
- [45] M. -M. Zhao, Q. Wu, M. -J. Zhao and R. Zhang, "Intelligent Reflecting Surface Enhanced Wireless Network: Two-Timescale Beamforming Optimization," in *IEEE Transactions on Wireless Communications*, doi: 10.1109/TWC.2020.3022297.
- [46] B. Fang, Z. Qian, W. Zhong and W. Shao, "Iterative precoding for MIMO wiretap channels using successive convex approximation," 2015 IEEE 4th

Asia-Pacific Conference on Antennas and Propagation (APCAP), Kuta, 2015, pp. 65-66, doi: 10.1109/APCAP.2015.7374273.

[47] Y. Guo, "Alternative optimization of multi-objective reservoirs with fuzzy optimum neural networks," 2017 13th International Conference on Natural Computation, Fuzzy Systems and Knowledge Discovery (ICNC-FSKD), Guilin, 2017, pp. 1327-1330, doi: 10.1109/FSKD.2017.8392958.

[48] J. Liu, K. Xiong, D. W. K. Ng, P. Fan, Z. Zhong and K. B. Letaief, "Max-Min Energy Balance in Wireless-Powered Hierarchical Fog-Cloud Computing Networks," in IEEE Transactions on Wireless Communications, doi: 10.1109/TWC.2020.3007805.

[49] C. Wang, H. Wang, D. W. K. Ng, X. Xia and C. Liu, "Joint Beamforming and Power Allocation for Secrecy in Peer-to-Peer Relay Networks," in IEEE Transactions on Wireless Communications, vol. 14, no. 6, pp. 3280-3293, June 2015, doi: 10.1109/TWC.2015.2403367.

[50] J. Zhang, J. Han, L. Xiang, D. W. K. Ng, M. Chen and M. Jo, "On the Performance of LTE/Wi-Fi Dual-Mode Uplink Transmission: Connection Probability versus Energy Efficiency," in IEEE Transactions on Vehicular Technology, doi: 10.1109/TVT.2020.3007922.

[51] M. Bengtsson and B. Ottersten, "Optimal and suboptimal transmit beamforming," Handbook of antennas in wireless communications, Boca Raton, FL: CRC, 2001.

[52] J. Li, P. Stoica and T. Yardibi, "Covariance beamforming, covariance matrix tapers and matrix beamforming are related," in Electronics Letters, vol. 44, no. 5, pp. 383-384, 28 Feb. 2008, doi: 10.1049/el:20083103.

[53] U. Hamid, R. A. Qamar and K. Waqas, "Performance comparison of time-domain and frequency-domain beamforming techniques for sensor array processing," Proceedings of 2014 11th International Bhurban Conference on Applied

Sciences & Technology (IBCAST) Islamabad, Pakistan, 14th - 18th January, 2014, Islamabad, 2014, pp. 379-385, doi: 10.1109/IBCAST.2014.6778172.

[54] J. Chen, Y. Liang, Y. Pei and H. Guo, "Intelligent Reflecting Surface: A Programmable Wireless Environment for Physical Layer Security," in *IEEE Access*, vol. 7, pp. 82599-82612, 2019, doi: 10.1109/ACCESS.2019.2924034.

[55] X. Liu, Y. Wang, F. Zhou, S. Ma, R. Q. Hu and D. W. K. Ng, "Beamforming Design for Secure MISO Visible Light Communication Networks with SLIPT," in *IEEE Transactions on Communications*, doi: 10.1109/TCOMM.2020.3019818.

[56] J. Liu, K. Xiong, D. W. K. Ng, P. Fan and Z. Zhong, "Optimal Design of Wireless-Powered Hierarchical Fog-Cloud Computing Networks," 2019 *IEEE Global Communications Conference (GLOBECOM)*, Waikoloa, HI, USA, 2019, pp. 1-6, doi: 10.1109/GLOBECOM38437.2019.9013868.

[57] E. Avventi, "Divergence-based spectral approximation with degree constraint as a concave optimization problem," 2008 47th *IEEE Conference on Decision and Control*, Cancun, 2008, pp. 732-737, doi: 10.1109/CDC.2008.4739208.

[58] R. Ji, Y. Liang, L. Xu and W. Zhang, "A Concave Optimization-Based Approach for Joint Multi-Target Track Initialization," in *IEEE Access*, vol. 7, pp. 108551-108560, 2019, doi: 10.1109/ACCESS.2019.2933650.

[59] B. yonesie, A. Sebghati and S. Shamaghdari, "Control Design by Convex-Concave Optimization for Flow Rate Control Process," *Electrical Engineering (ICEE), Iranian Conference on*, Mashhad, 2018, pp. 869-874, doi: 10.1109/ICEE.2018.8472648.

[60] X. Zhou, S. Yan, Q. Wu, J. Lin and F. Shu, "Robust Beamforming Design for Secure DM-Based Relay Networks with Self-Sustained Jammers," in *IEEE Access*, vol. 7, pp. 969-983, 2019, doi: 10.1109/ACCESS.2018.2886079.

- [61] Y. Yang, M. Pesavento, S. Chatzinotas and B. Ottersten, "Successive Convex Approximation Algorithms for Sparse Signal Estimation with Nonconvex Regularizations," in *IEEE Journal of Selected Topics in Signal Processing*, vol. 12, no. 6, pp. 1286-1302, Dec. 2018, doi: 10.1109/JSTSP.2018.2877584.
- [62] Z. Li, L. Chen, X. Chen and W. Wang, "Beamforming in Distributed Antenna Systems Based on Successive Convex Approximation and Dual Decomposition," 2019 11th International Conference on Wireless Communications and Signal Processing (WCSP), Xi'an, China, 2019, pp. 1-6, doi: 10.1109/WCSP.2019.8928044.
- [63] A. Liu, V. K. N. Lau and M. Zhao, "Online Successive Convex Approximation for Two-Stage Stochastic Nonconvex Optimization," in *IEEE Transactions on Signal Processing*, vol. 66, no. 22, pp. 5941-5955, 15 Nov.15, 2018, doi: 10.1109/TSP.2018.2871389.
- [64] K. Wang, Q. Wu, W. Chen, Y. Yang and D. W. K. Ng, "Energy-Efficient Buffer-Aided Relaying Systems With Opportunistic Spectrum Access," in *IEEE Transactions on Green Communications and Networking*, vol. 4, no. 3, pp. 731-744, Sept. 2020, doi: 10.1109/TGCN.2020.2977345.
- [65] H. Wang, C. Wang and D. W. K. Ng, "Artificial Noise Assisted Secure Transmission Under Training and Feedback," in *IEEE Transactions on Signal Processing*, vol. 63, no. 23, pp. 6285-6298, Dec.1, 2015, doi: 10.1109/TSP.2015.2465301.
- [66] X. Zhou et al., "Secure SWIPT for Directional Modulation-Aided AF Relaying Networks," in *IEEE Journal on Selected Areas in Communications*, vol. 37, no. 2, pp. 253-268, Feb. 2019, doi: 10.1109/JSAC.2018.2872372.
- [67] Y. Sun, D. Xu, D. W. K. Ng, L. Dai and R. Schober, "Optimal 3D-Trajectory Design and Resource Allocation for Solar-Powered UAV Communication Systems," in *IEEE Transactions on Communications*, vol. 67, no. 6, pp. 4281-4298, June 2019, doi: 10.1109/TCOMM.2019.2900630.

[68] D. Xu, Y. Sun, D. W. K. Ng and R. Schober, "Multiuser MISO UAV Communications in Uncertain Environments With No-Fly Zones: Robust Trajectory and Resource Allocation Design," in *IEEE Transactions on Communications*, vol. 68, no. 5, pp. 3153-3172, May 2020, doi: 10.1109/TCOMM.2020.2970043.

[69] Q. Wu and R. Zhang, "Beamforming Optimization for Intelligent Reflecting Surface with Discrete Phase Shifts," *ICASSP 2019 - 2019 IEEE International Conference on Acoustics, Speech and Signal Processing (ICASSP)*, Brighton, United Kingdom, 2019, pp. 7830-7833, doi: 10.1109/ICASSP.2019.8683145.

[70] S. Boyd and L. Vandenberghe, *Convex optimization*. Cambridge university press, 2004.

[71] X. Sun, C. Shen, D. W. K. Ng and Z. Zhong, "Robust Trajectory and Resource Allocation Design for Secure UAV-Aided Communications," *2019 IEEE International Conference on Communications Workshops (ICC Workshops)*, Shanghai, China, 2019, pp. 1-6.

[72] Derrick Wing Kwan Ng; Trung Q. Duong; Caijun Zhong; Robert Schober, "The Era of Wireless Information and Power Transfer," in *Wireless Information and Power Transfer: Theory and Practice*, Wiley, 2019, pp.1-16, doi: 10.1002/9781119476863.ch1.

[73] S. Leng, D. W. K. Ng, N. Zlatanov and R. Schober, "Multi-objective beamforming for energy-efficient SWIPT systems," *2016 International Conference on Computing, Networking and Communications (ICNC)*, Kauai, HI, 2016, pp. 1-7, doi: 10.1109/ICCNC.2016.7440679.

[74] S. Hu, Z. Wei, Y. Cai, D. W. K. Ng, J. Yuan, "Sum-Rate Maximization for Multiuser MISO Downlink Systems with Self-sustainable IRS," *2020 IEEE Global Commun. Conf. (GLOBECOM)*, 2020, arXiv: 2005.11663.

Appendix

In order to proof the SDR is tight, the Lagrange dual function must be used. But first and foremost, it is obviously that when the $\mathcal{C}_k \leq 0$, the optimal $\mathbf{w}_k^* = 0$ for each user which means $\text{rank}(\mathbf{W}_k^*) = 0$. For $\mathcal{C}_k > 0$, the rank-one property is able to be presented.

According to (5), the constraint C2 can be rewritten as:

$$\begin{aligned} C2 = \gamma_k \left[\sum_{i \neq k}^N \text{Tr}[\mathbf{W}_i (\mathbf{H}_{r,k}^H \mathbf{u} \mathbf{u}^H \mathbf{H}_{r,k} + \mathbf{H}_{d,k}^H \mathbf{H}_{d,k})] + n_k^2 \right] \\ - \text{Tr}[\mathbf{W}_k (\mathbf{H}_{r,k}^H \mathbf{u} \mathbf{u}^H \mathbf{H}_{r,k} + \mathbf{H}_{d,k}^H \mathbf{H}_{d,k})] \leq 0 \end{aligned} \quad (11)$$

We can formulate the Lagrange dual function in terms of the \mathbf{W}_k based on (P7) as following.

$$\begin{aligned} \mathcal{L}(\mathbf{W}_k, \mathbf{Y}_k, \lambda_1, \lambda_2) \\ = F_1(\mathbf{W}_k) - F_2(\mathbf{W}_k^i) - \text{Tr} \left[\left(\nabla_{\mathbf{W}_k} F_2(\mathbf{W}_k^i) \right)^H (\mathbf{W}_k - \mathbf{W}_k^i) \right] \\ + \lambda_1 \left[\sum_k \text{Tr}(\mathbf{W}_k) - P_{max} \right] \\ + \lambda_2 \left\{ \gamma_k \left[\sum_{i \neq k}^N \text{Tr}[\mathbf{W}_i (\mathbf{H}_{r,k}^H \mathbf{u} \mathbf{u}^H \mathbf{H}_{r,k} + \mathbf{H}_{d,k}^H \mathbf{H}_{d,k})] + n_k^2 \right] \right. \\ \left. - \text{Tr}[\mathbf{W}_k (\mathbf{H}_{r,k}^H \mathbf{u} \mathbf{u}^H \mathbf{H}_{r,k} + \mathbf{H}_{d,k}^H \mathbf{H}_{d,k})] \right\} \\ - \text{Tr}(\mathbf{W}_k \mathbf{Y}_k) \end{aligned} \quad (12)$$

where λ_1 , λ_2 , \mathbf{Y}_k are the Lagrange multiplier scalar and Lagrange multiplier matrix associated with constraints of C1, C2 and C3 respectively [3]. Then, the Lagrange dual problem would be formulated as:

$$\min_{\mathbf{Y}_k \succeq \mathbf{0}, \lambda_1 \geq 0, \lambda_2 \geq 0} \max_{\mathbf{W}_k} \mathcal{L}(\mathbf{W}_k, \mathbf{Y}_k, \lambda_1, \lambda_2) \quad (13)$$

Next, we are able to concentrate on the KKT conditions [70].

<p>K1: $\mathbf{Y}_k^* \succcurlyeq \mathbf{0}, \lambda_1^* \geq 0, \lambda_2^* \geq 0$</p> <p>K2: $\mathbf{W}_k^* \mathbf{Y}_k^* = \mathbf{0}$</p> <p>K3: $\nabla_{\mathbf{W}_k^*} \mathcal{L} = 0$</p>

Expand the K3 by calculating the derivative of (10), we got:

$$\begin{aligned}
\mathbf{Y}_k^* &= \nabla_{\mathbf{W}_k} F_1(\mathbf{W}_k) - 2 \left(\nabla_{\mathbf{W}_k} F_2(\mathbf{W}_k^i) \right) + \lambda_1^* \mathbf{I}_N - \lambda_2^* (\mathbf{H}_{r,k}^H \mathbf{u} \mathbf{u}^H \mathbf{H}_{r,k} + \mathbf{H}_{d,k}^H \mathbf{H}_{d,k}) \\
&= \lambda_1^* \mathbf{I}_N + \nabla_{\mathbf{W}_k} F_1(\mathbf{W}_k) - 2 \left(\nabla_{\mathbf{W}_k} F_2(\mathbf{W}_k^i) \right) - \lambda_2^* (\mathbf{H}_{r,k}^H \mathbf{u} \mathbf{u}^H \mathbf{H}_{r,k} + \mathbf{H}_{d,k}^H \mathbf{H}_{d,k}) \quad (14)
\end{aligned}$$

For $\lambda_1^* \geq 0$, $\lambda_1^* \mathbf{I}_N$ is definitely full rank, and $\nabla_{\mathbf{W}_k} F_1(\mathbf{W}_k) \succcurlyeq \mathbf{0}$, then $\lambda_1^* \mathbf{I}_N + \nabla_{\mathbf{W}_k} F_1(\mathbf{W}_k)$ must be full rank. We then define a matrix $\mathcal{M} = 2 \left(\nabla_{\mathbf{W}_k} F_2(\mathbf{W}_k^i) \right) + \lambda_2^* (\mathbf{H}_{r,k}^H \mathbf{u} \mathbf{u}^H \mathbf{H}_{r,k} + \mathbf{H}_{d,k}^H \mathbf{H}_{d,k})$. Hence, \mathbf{Y}_k^* is represented as:

$$\mathbf{Y}_k^* = \lambda_1^* \mathbf{I}_N + \nabla_{\mathbf{W}_k} F_1(\mathbf{W}_k) - \mathcal{M} \quad (15)$$

According to K2, it can be concluded that if \mathbf{Y}_k^* has full rank which means $\text{Rank}(\mathbf{Y}_k^*) = N$, then there is only when $\text{Rank}(\mathbf{W}_k^*) = 0$ can satisfy K2. However, if $P_{max} > 0$, $\text{Rank}(\mathbf{W}_k^*)$ could not be zero. Then, the only solution that can satisfy K2, is making \mathbf{Y}_k^* not full rank, and \mathbf{W}_k sits in the null-space of \mathbf{Y}_k^* . To start with, the maximum eigen value of \mathcal{M} is defined as $\lambda_{\mathcal{M}}^{max}$. If $\lambda_{\mathcal{M}}^{max} > \lambda_1^*$, then according to (13), $\mathbf{Y}_k^* \succcurlyeq \mathbf{0}$ cannot be met. And if $\lambda_{\mathcal{M}}^{max} < \lambda_1^*$, \mathbf{Y}_k^* would be a semidefinite matrix with full rank which makes K2 not hold. Thus, $\lambda_{\mathcal{M}}^{max}$ should be equals to λ_1^* , then $\text{Rank}(\mathbf{Y}_k^*) = N - 1$. In result, we can conclude that $\text{Rank}(\mathbf{W}_k^*) \leq 1$. Therefore, when $P_{max} > 0$ and K1, K2 and K3 are all satisfied, \mathbf{W}_k^* is indeed a rank one matrix.